

Selective Stiffening in Soft Actuators by Triggered Phase Transition of Hydrogel-Filled Elastomers

Francesco Visentin,* Saravana Prashanth Murali Babu, Fabian Meder, and Barbara Mazzolai*

Nature has inspired a new generation of robots that not only imitate the behavior of natural systems but also share their adaptability to the environment and level of compliance due to the materials used to manufacture them, which are typically made of soft matter. In order to be adaptable and compliant, these robots need to be able to locally change the mechanical properties of their soft material-based bodies according to external feedback. In this work, a soft actuator that embodies a highly controllable thermo-responsive hydrogel and changes its stiffness on direct stimulation is proposed. At a critical temperature, this stimulation triggers the reversible transition of the hydrogel, which locally stiffens the elastomeric containment at the targeted location. By dividing the actuator into multiple sections, it is possible to control its macroscopic behavior as a function of the stiffened sections. These properties are evaluated by arranging three actuators into a gripper configuration used to grasp objects. The results clearly show that the approach can be used to develop soft actuators that can modify their mechanical properties on-demand in order to conform to objects or to exert the required force.

perform complex tasks^[17–19] while withstanding large deformations without damage.^[20] In addition, by mimicking humans and other living organisms, such bioinspired robots can be used to study and verify theories derived from their observations.^[21–24]

Various actuation strategies have already been used to perform such complex tasks. However, even when they are arranged correctly, the actuators alone might not be able to ensure that the robot adapts and deforms effectively. Materials also play an important role, for example by reversibly changing their mechanical properties according to the external feedback received.

In nature there are several examples of soft bodies that change their stiffness in order to adapt to the environment (Figure 1A). Octopuses, for example, have a completely soft body with no rigid structures.

However, they can selectively stiffen a section of their body and change their morphology or exert the required force in order to perform specific tasks or patterns of movements.^[25] Similarly, plants can locally fill their cells with water to produce turgor pressure. This enables them to rotate, lift, or move their parts.^[26] Replicating such a feature in a soft robot opens the way to a new class of machines that can tune their functionalities and behaviors to better adapt to the surroundings.

One of the most effective solutions inspired by this remarkable property is the use of unidirectional stretchable fibers^[27,28] embedded into a soft structure. These provide controllable and repeatable motions. However, they do not enable on-demand tunability since the fibers cannot be reconfigured once embedded into the structure.

Reconfigurability is possible using low melting point materials.^[29] Shape-memory alloys and polymers^[30] are good candidates since they can be precisely embedded and locally controlled. Alternatively, magneto- and electrorheological fluids^[31–33] provide high forces, however their life-span may be short due to the continuous deposition of the particles in suspension. Another solution is to use external sources, such as magnetic or electrostatic fields^[34,35] or the mechanical lock of internal components through tensioning wires.^[17,36]


A common actuation technique in soft robotics to achieve variable stiffness is based on jamming, in which materials – either consisting of particles or sheets – change from being flexible to a solid-like state by increasing the packing density. By controlling the level of aggregation of the material (e.g., by varying the internal pressure of the jamming compartments),

1. Introduction

The idea of robots is no longer only linked to rigid machines made of hard materials – such as steel or aluminum – that can be precisely controlled and replicate tasks with a high accuracy. A new approach is now rapidly changing the concept of robots^[1,2] by exploiting soft, elastic, and flexible materials to adapt to complex unstructured environments.^[3,4] Thanks to their compliant structure, these robots can passively conform to arbitrary geometries,^[5] safely interact with humans,^[6,7] and manipulate fragile objects.^[8,9] They can also perform multiple gaits both on irregular surfaces^[10–13] and in water,^[14–16] and

Dr. F. Visentin, S. P. Murali Babu, Dr. F. Meder, Dr. B. Mazzolai
Bioinspired Soft Robotics Laboratory
Istituto Italiano di Tecnologia
Pontedera 56025, Italy
E-mail: francesco.visentin@iit.it; barbara.mazzolai@iit.it

S. P. Murali Babu
Scuola Superiore Sant'Anna
The BioRobotics Institute
Pontedera 56025, Italy

 The ORCID identification number(s) for the author(s) of this article can be found under <https://doi.org/10.1002/adfm.202101121>.

© 2021 The Authors. Advanced Functional Materials published by Wiley-VCH GmbH. This is an open access article under the terms of the Creative Commons Attribution License, which permits use, distribution and reproduction in any medium, provided the original work is properly cited.

DOI: 10.1002/adfm.202101121

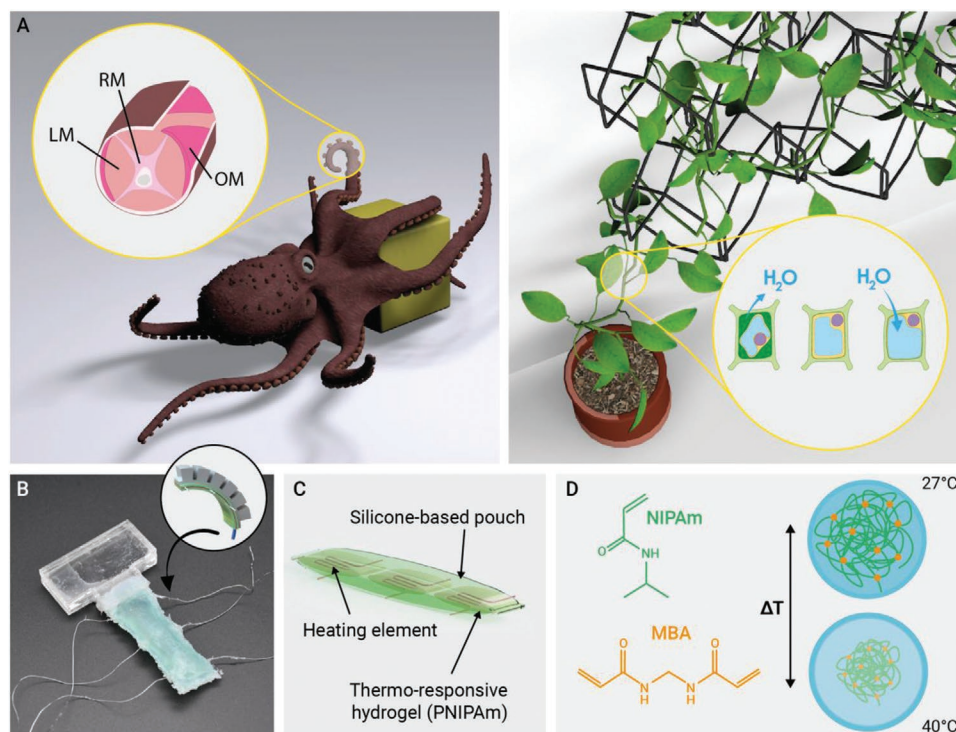


Figure 1. Variable stiffening for soft actuators. A) Examples from nature of stiffness changing. An octopus can change the configuration of its arm by combining the contraction of the different muscles (LT: longitudinal muscle, RM: radial muscle, OB: oblique muscle). A plant can change the stiffness of its cells also by regulating the amount of water it contains. Replicating these functionalities in a soft actuator, increases its adaptability and functionalities. B) The proposed thermo-responsive, hydrogel-filled reinforced layer used in combination with a PneuNet actuator. C) Internal structure of the reinforced layer containing the PNIPAm hydrogel and a set of zigzag-shaped coils used to trigger the phase change. D) Chemical structure of the hydrogel (PNIPAm and MBA as cross-linkers) and its thermal behavior. Upon crossing the LCST, the demixing phase transition occurs which transforms the polymer chains into smaller globules.

a different level of stiffness of an actuator or of a part of a soft robot is possible.^[37–41] The main drawback of this jamming-based approach is the high complexity needed to obtain the localized stiffening as this requires a complex tubing and valve system to control each of the compartments.^[42]

To enable soft robots to exhibit locally-controlled mechanical properties, solutions are needed that enable locally-controlled and reversible changes in the elastic properties of the robot's structural materials. A solution can be found in the works related to stretchable electronics which use spatioselective ultraviolet exposure to locally alter the mechanical properties of pre-treated polymer substrates.^[43–45] The approach allows to increase the Young's modulus of the stiffened area more than 100-fold compared to the untreated area. Reversible alteration of the stiffness can be achieved by selective heating instead of ultraviolet exposure. Another possible approach is to selectively changing the mechanical properties of the soft material which can be programmed to react to external stimuli such as light or magnetic field.^[46,47] While these methods allow for the development miniaturized, controllable, soft robots they also require to have an external source to trigger the different behaviors that might limit the integrability of the principle in the soft device. Here, we propose a controllable, soft robotic actuator based on a hydrogel that can reversibly change its stiffness in response to thermal stimuli that can be triggered by a simple, embeddable heating system. We used a poly(*N*-isopropylacrylamide)

(PNIPAm) hydrogel as an inextensible layer of a PneuNet (pneumatic networks) bending actuator,^[48,49] selectively activated in response to localized heating (Figures 1B,C). PNIPAm hydrogels are a well-known class of thermo-responsive materials that undergo a lower critical solution temperature (LCST) demixing, coil-to-globule, and phase transition.^[50] These hydrogels exhibit large conformational changes leading to an expansion or contraction of the network as a consequence of external stimuli. When heated above the LCST, the hydrogen bonds between the polar groups of the polymer and the water molecules break (Figure 1D). The water is released from the network, which results in a change from a swollen hydrated state to a shrunken dehydrated state, losing about 90% of its volume.^[51] In addition to the variation in viscosity, the material changes from being transparent in the visible light range to highly turbid.^[52,53] Due to their particular properties, these materials are used for a range of applications including drug delivery systems,^[54,55] switchable electronics,^[56] bio-sensors,^[57,58] actuators,^[59] and responsive surfaces.^[60,61]

Through an integrated design and manufacturing process, straightforward embodiments of these actuators have been demonstrated creating a “jamming effect” without the need for additional external pumps. Simply filling the soft body with the hydrogel, whose properties can be controlled to create selective stiffening produces a macroscopic stiffness variation controlling the mechanical properties in soft robots in situ. Differently

from the current phase changing soft actuators our approach does not depend on external sources (i.e., light, laser, or magnetic field) but only requires an integrated heating systems that is used to create selective stiffening to better conform to different-shape objects, or to exert the required force.

To validate the approach, we characterized the mechanical response of the hydrogel, both alone and when it is used as filler in a soft structure. We verified the approach by developing a soft actuator that shows different properties according to the amount and location of the activated hydrogel, and which can be used both in a standalone, as a gripper configuration, or in an underwater application.

2. Results

2.1. Responsive Hydrogel Synthesis and Characterization

The hydrogel was prepared following the protocol in Ref. [53] using a surfactant-free radical polymerization of the monomer *N*-isopropylacrylamide (NIPAm) and the cross-linker *N,N'*-methylene-bis-acrylamide (MBA) in water (Figure 1C). Further details are given in the Materials and Methods section.

MBA enables the growth of branched polymer chains from the NIPAm monomers creating long PNIPAm chains and complex 3D networks. The amount of cross-linker thus changes the microscopic architecture of the hydrogel, and influences its macroscopic behavior. A PNIPAm hydrogel with a low amount of cross-linker swells more and has a low viscosity due to the lower rigidity of the network.^[53,62] We used a 10 wt% concentration ratio of the monomer, which provided good results for the proposed application. Figure S1, Supporting Information shows the calorimetrically determined phase transition and the critical point of the synthesized hydrogel.

The synthesized hydrogel is viscoelastic with both viscous and elastic components in its stress response (Figure S2, Supporting Information). This means that upon application of an external load, the material first stretches elastically, then starts to flow and move within the container. Being elastic also means that

the hydrogel recovers its original state when the external load is removed. We identified the viscosity and elasticity modules and found an almost 200-fold increase in the elasticity of the activated hydrogel (@40 °C, 5.97×10^4 Pa) compared to the non-activated hydrogel (@27 °C, 3.08×10^2 Pa). Similarly, the phase transition resulted in a 49-fold increase in the viscosity between the activated (6.75×10^3 Pa) and non-activated state (1.35×10^2 Pa).

We further validated the mechanical properties of the hydrogel by performing an indentation test, measuring the force needed to penetrate 12 mm into 20 mL of PNIPAm hydrogel at a 5 mm s^{-1} speed either before or after the phase change of the material. The results showed that for the non-activated hydrogel, the maximum measured force was 0.10 N, while in its activated state, the maximum force was 1.08 N. In fact, the stiffness increased more than 10 times when the hydrogel was activated (Figure 2A). We evaluated the effect of hydrogel composition on the heat-induced stiffness variation by varying the concentration of the monomer (2.5, 5, 10, and 15 wt%) and maintaining a fixed water volume and cross-linker concentration. (Figure S3, Supporting Information).

To control the phase transition, we investigated various methods: using an external heat source; direct Joule heating; and heat transfer obtained by separating the hydrogel from the Joule heating source with a thin layer (2 mm) of silicone rubber (Ecoflex 00–30, Smooth-On). As an external source, we used a heat gun (EOTO202, RS PRO, RS Components Ltd), while for the joule heating, we applied 0.5 A to a Nichrome wire. The external heat source was the fastest but the least controllable solution, since it was not able to accurately focus on a specific spot and it also increased the temperature of the container (Movie S1, Supporting Information). Direct Joule heating, on the other hand, was the most effective since the phase transition was well localized around the heating coil (Figure 2B).

2.2. Characterization of Hydrogel-Filled Elastomers

Many soft robots are made of soft, hyper-elastic materials (from below Shore A hardness, 00–10, and up to 80 A) which enable

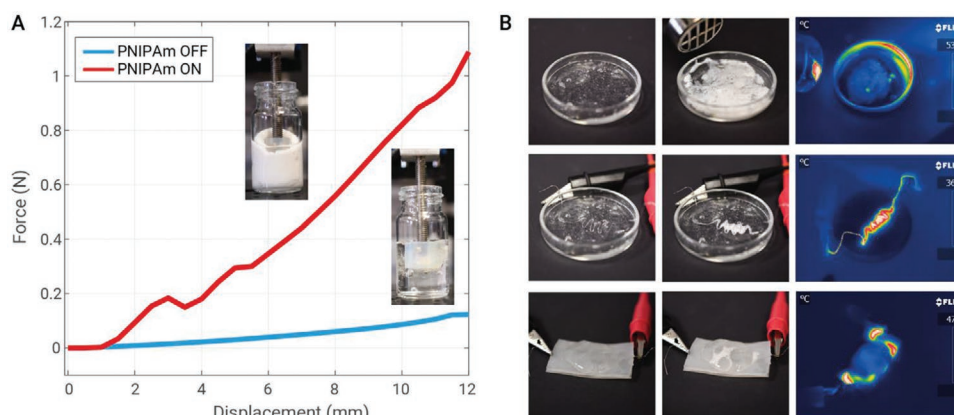


Figure 2. PNIPAm phase change behavior. A) Indentation test to evaluate the change in properties between the two phases of the hydrogel. When activated, a force of 1.08 N is required to indent 12 mm of the hydrogel. The same displacement in the non-activated state requires a force more than 10 times lower than 0.10 N. B) Different methods for performing the phase transition. From top to bottom: external heating, direct Joule heating, and heat transfer by adding a 2 mm layer of silicone rubber between the heating coil and the hydrogel. In all the cases, the status of the hydrogel before and after the phase transition is shown. The thermal image was acquired in its activated state.

higher adaptability and flexibility compared to classical rigid-link robots.^[63] However, the set of possible deformations can be defined by embedding inextensible components in pre-defined bending points. To extend the functionalities of such robots localized, controllable stiffening of the material that the robot is made of is needed. The particular properties of the PNIPAm hydrogel make it suitable for use as a tunable, filler material of a soft structure.

We injected the hydrogel as a tunable filler material into containers of these elastomers. To verify the stiffening properties

of the PNIPAm hydrogel, and to guide the design parameters of the actuator, we tested the performance of a cylindrical structure upon an applied load.

A series of cylindrical soft structures (Ecoflex 00–30A, Smooth-on) were manufactured with different wall thicknesses (1, 2, 3, and 5 mm) (Table S1, Supporting Information). Compression tests were performed with a total displacement of 10 mm at a constant speed (0.5 mm s^{-1}). We then measured the reaction force of the structures when filled

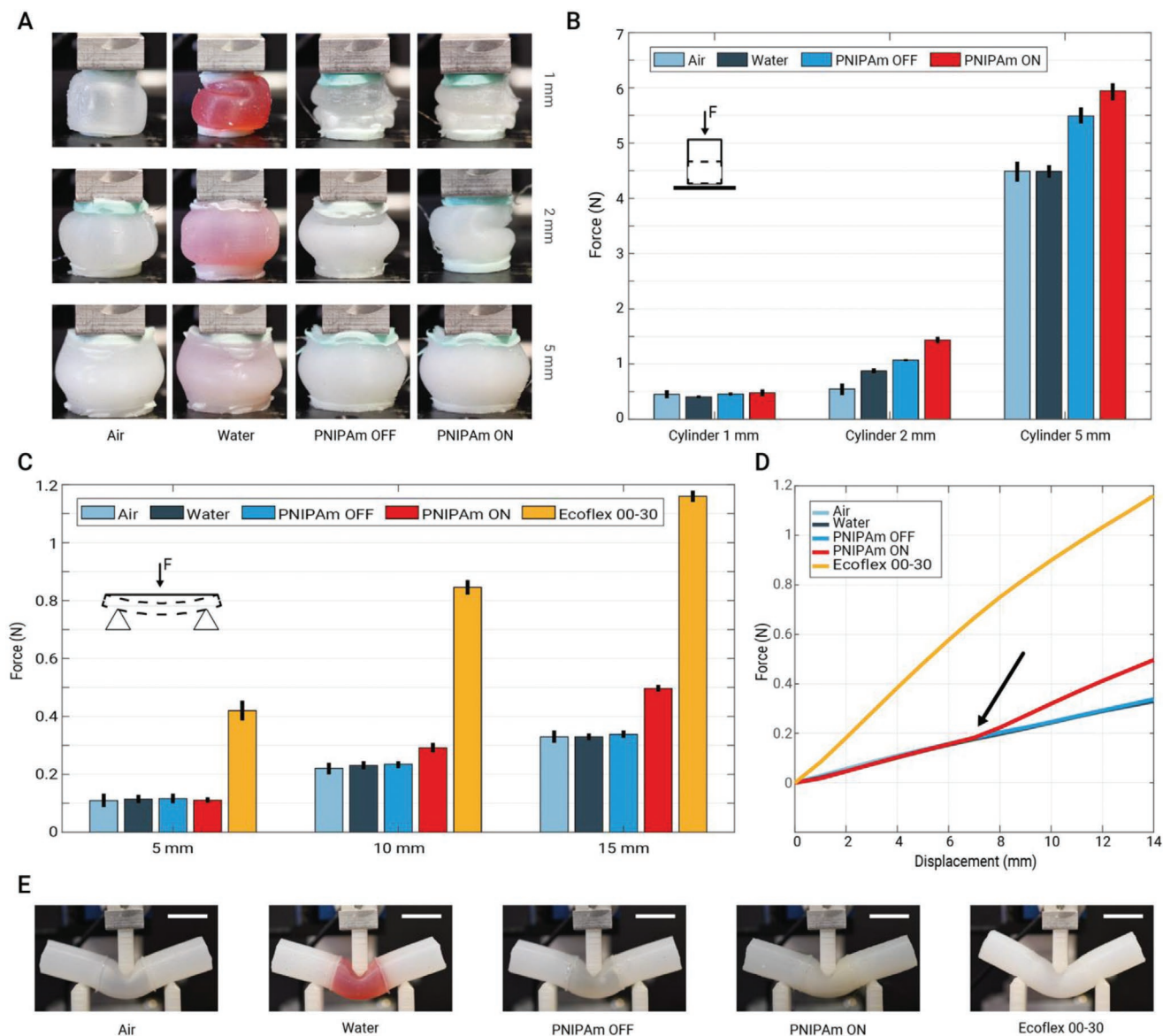


Figure 3. PNIPAm-filled elastomers as a way to locally control stiffening in soft robots. A) Highlight of the compression tests. By increasing the wall thickness of the elastic cylinder containing the fillers, the deformation is more controlled and uniform. B) Compression test of the elastic cylinders with different fillers: air, water, and PNIPAm. Force exerted by a soft cylindrical structure when filled with air, water, or PNIPAm. On average, for all the cases, the non-activated PNIPAm hydrogel performed 1.7 and 1.2× better than air and water, respectively. When activated, on average it performed 2 and 1.5× better than air and water, respectively. C) Results of the flexural analysis of a soft beam filled with air, water, PNIPAm, or silicone rubber (Ecoflex 00–30, Smooth-On). As expected, the silicone rubber-filled beam showed the highest resistance to bending (flexural modulus 0.0095 MPa), but it cannot be controlled. In its non-activated state, PNIPAm hydrogel showed 27% of the flexural modulus of silicone rubber, and an increase of up to 36% when activated. D) Flexural analysis of the structures as a function of the various fillers. Activated PNIPAm behaves similarly to water and air until the indentation is half the thickness of the soft bar, then it linearly increases the resistance force. E) The structures at 15 mm indentation during flexural analysis. The dimension bar is the same size as the indenter (20 mm).

with the same volume of air, water, and PNIPAm hydrogel (Figure 3A).

The phase transition in the hydrogel was obtained by Joule heating using a current of 0.5 A applied for 30 s to a planar, zigzag coil-shaped flexible Nichrome wire embedded into the structures. Upon visible phase change, the current was reduced to 0.3 A for the rest of the experiment. As expected, the increase in the wall thickness led to an increase in the resulting force (Figure 3B).

Regarding the filler, air was the least effective material as its compressibility caused a large variability in measurements. The use of water as filler provided good results; however, to control its phase change, the system has to be below melting point (0 °C), which requires a large amount of energy.

PNIPAm hydrogel always performed better than water and air due to its intermediate state between solids and liquids.^[64] The resulting forces were in general higher when the hydrogel was in the activated state compared to the non-activated state. Considering structures filled with air as a reference, water-filled structures on average provided a 22% increase in stiffening, non-activated hydrogel-filled structures provided 51.8%, and activated hydrogel-filled structures provided 69.33%, respectively. If water-filled structures were considered as a reference, non-activated hydrogel-filled structures provided a 22.8% increase in stiffening, and activated hydrogel-filled structures provided 35.6%, respectively. However, between the non-activated and activated state of the hydrogel-filled structures, there is a 76.7% increase in stiffening. Among the considered cases, structures with a 2 mm wall thickness of the outer silicone elastomer provided the largest force variation (86.2%) between the non-activated and activated state of the PNIPAm hydrogel. We thus used this wall thickness as a design parameter to manufacture the controllable soft actuator.

We further investigated the effect of the temperature variation on stiffness of the hydrogel. As in the previous experiments, we applied 0.5 A to the hydrogel upon reaching a desired temperature. Then we compressed the 3 mm cylinder with a total displacement of 10 mm at a constant speed (0.5 mm s⁻¹). Results (Figure S4, Supporting Information) show that by increasing the temperature close to the LCST of the hydrogel the stiffness of the material gradually increases providing initially a force of 2.4 N in the non-activated state up to 3.1 N when heated up to 35.2 °C

In addition to the compression analysis, we tested the performance of the different fillers in a standard three-point flexural test (Figure 3C). This information shows how well the materials resist bending, which is a fundamental property in the design of an actuator for soft robotics. The cylindrical shape (Ecoflex 00–30, Smooth-on) is a single structure with a central hollow chamber with a wall thickness of 2 mm (Table S2, Supporting Information). We assessed the flexural modulus of the structure when filled with air, water, PNIPAm hydrogel, and Ecoflex 00–30. In each measurement, the probe performed a total displacement of 15 mm at a constant speed (5 mm s⁻¹).

The results showed that air-, water-, and non-activated PNIPAm hydrogel-filled structures have a very similar flexural modulus (0.0026 MPa), which is 27% of the modulus of the pure silicone rubber (0.0095 MPa). In its activated state, instead, the PNIPAm hydrogel-filled structure showed a sig-

nificantly higher flexural modulus (0.0035 MPa, 36% of silicone rubber) with a 74% increase in stiffness with respect to the non-activated case.

PNIPAm-filled structures behaved similarly to the other fillers (air, water) up to about 50% compression, after which they had a higher force response (Figure 3D). The results showed that for a displacement that is lower than half of the cylinder radius, all structures, except for the fully silicone rubber-filled structure, have low bending resistance (Figure 3E).

We can thus conclude that the use of the PNIPAm as a filler does not influence the passive adaptability of its elastic container and, when activated, provides high bending resistance under larger displacement.

2.3. Design and Performance of the Variable Stiffness Actuator

PneuNets are a well-known class of actuators for soft robotics.^[48] They consist in a series of channels and chambers inside an elastomer which expand towards the least stiff region when pressurized. By tuning the wall thickness of the base of the structure, or by adding an inextensible layer, the actuator can generate a unidirectional, reversible bending motion.

We aimed to expand the functionality of the actuator by replacing the passive inextensible layer with an active, locally controllable layer filled with PNIPAm hydrogel-filled PneuNet base. By locally tuning the stiffness of the material, the overall behavior of the actuator can be controlled.

The first step consists in the design and manufacture of the active reinforced layer, which was designed as a pouch made from two thin layers (thickness, 0.5 mm) of silicone rubber (Ecoflex 00–20, Smooth-On) filled with the hydrogel. In all the cases presented, the temperature gradient controlling the phase transition was obtained by Joule heating of incorporated flexible Nichrome wires embedded into the structures (Figure 4A). External environmental conditions may affect triggering the phase change such as an increase of the temperature above the LCST of the hydrogel. Thus, we evaluated the effects of a temperature gradient induced by external stimuli in both cases when the hydrogel-filled elastomers were directly exposed to different external temperatures (from 20 to 50 °C) and humidity (30–50–70%). As expected, when the temperature increases above the LCST, the phase change of the hydrogel is triggered for both the tested configurations (Movie S2, Supporting Information). The use of the elastomeric container provides a more uniform heating and prevent the loss of volume of the hydrogel (<1.5%) since the container is sealed and the released water from the hydrogel remains confined. We also show that the actuator can be operated under water extending the possible application ranges.

We manufactured two types of active reinforced layers: (L1) with a single continuous chamber with three independent activation sections, and (L2) with three separate chambers with independent activation sections of the same total length (Figures S5 and S6, Supporting Information). In both cases, due to the low LCST of the hydrogel and the small amount of material used in the active reinforced layer, the phase transition happened in <20 s after the electrical current had been injected. However, to ensure a complete stiffening of each section, we kept the current flowing in the wire for at least 40 s (Movie S3,

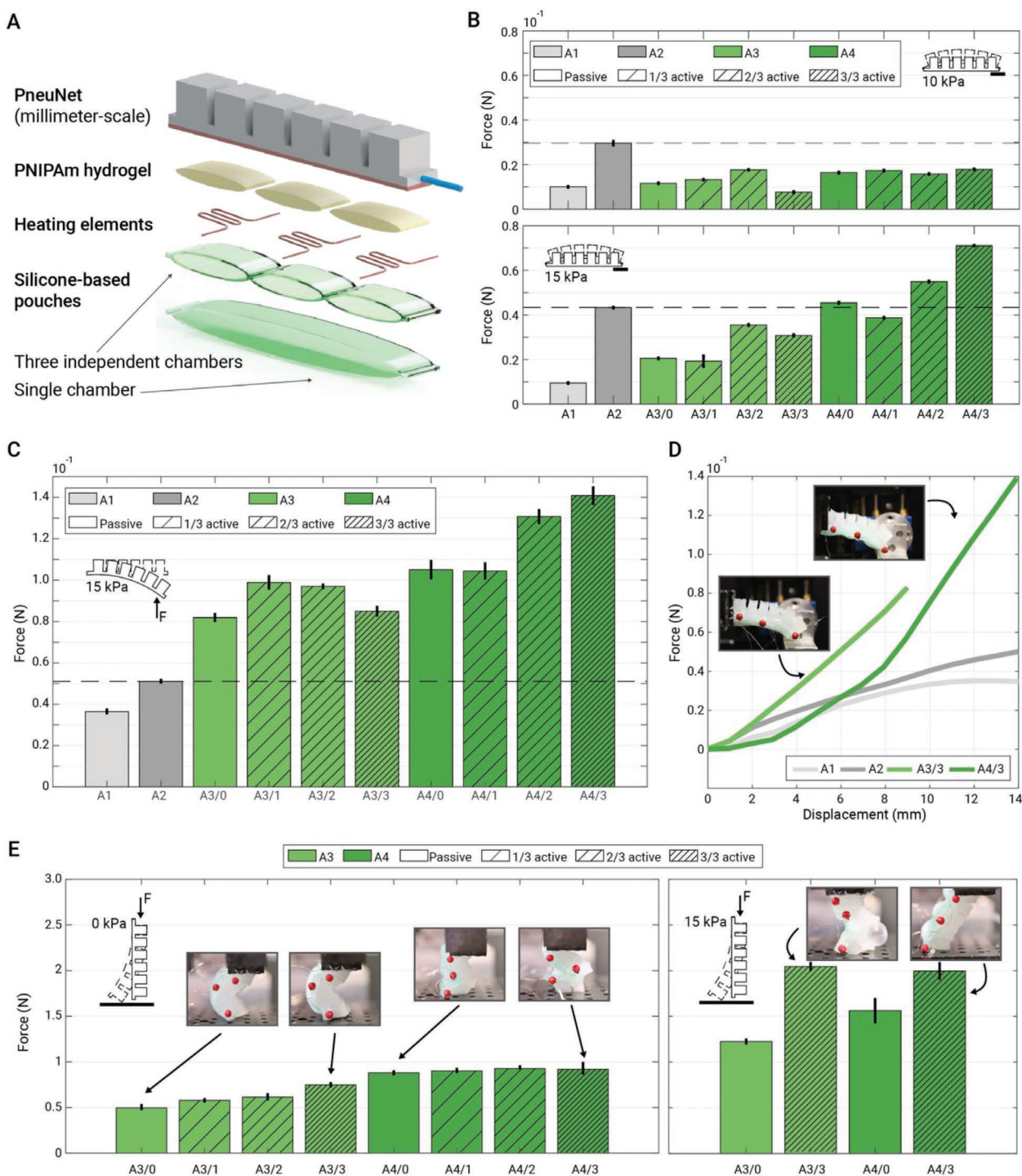


Figure 4. Design and performance of the locally controllable soft actuators. A) 3D design of the actuators and the locally controllable reinforced layers based on PNIPAm hydrogel. B) Block force response of the actuators when pressurized with 10 kPa (top) and 15 kPa (bottom). At a lower pressure, the reinforced PneuNet (A2) outperforms all the other actuators. By increasing the input pressure (15 kPa), the three-sectioned actuator (A4) shows similar results to A2 without activation of the sections. However, when the PNIPAm inextensible layer is activated, the actuators exert up to 64% higher forces than A2. C) Pulling force of the actuators when pressurized to about 15 kPa. Overall, the use of the PNIPAm inextensible layer provides up to 160% higher resistance to pulling forces compared to the classical textile-based inextensible layer, and up to 271% compared to structures without any inextensible layer. D) Stiffening as a function of the displacement of A1-4 when all sections of A3 and A4 are active. E) Results of the vertical compression test on the stiffened actuator, highlighting that the geometry of the inextensible layer plays a key role in absorbing the applied forces. This can be seen in the left panel by comparing the results for A3 and A4. In the first case, the sequential activation of the sections increases the absorbed forces. In A4 the design of the reinforced layer leads to a constant absorbed force since the spaces between the chambers act as hinge joints and enable the actuator to fold onto it. When all the sections of the actuators are activated, with the pressurization of the actuator, the resistance force becomes twice as high as when unpressurized.

Supporting Information). We estimated that to fully heat a single section of the L1 takes around 40 s, and the complete recovery of the original state requires around 42 s. Similarly, to heat up a section of the L2 requires 35 s, and the recovery process takes around 45 s. The values may increase or decrease, respectively, when more than one section is activated or the initial temperature of the materials is closer to its LCST value.

Before integrating the reinforced layer, it is important to have extensive knowledge of its properties in order to assess its contribution to the global behavior of the actuator. For each of the proposed designs, we evaluated the effects of the selective stiffening of the hydrogel-filled elastomers on the force needed to deform the structure (Figure S7, Supporting Information). In all the measurements, we sequentially activated each of the sections of the reinforced layer and pulled the structure upwards for 15 mm at a constant speed of 0.7 mm s^{-1} . The results showed that increasing the number of activated sections resulted in an increase in the resistance force. The values obtained were very similar for L1 and L2. However, L1 showed a 25-fold increase comparing the non-activated to the fully activated state (from 3 to 76 mN) versus an 8.6-fold increase found in L2 (from 10 to 86 mN). The lower force of L2 might be due to the natural compliance of L2 in which the spaces between the chambers act as passive hinge joints.

We then evaluated the performance of the active reinforced layers when integrated into a soft actuator. To do this, we designed and manufactured a series of PneuNets with the same channel and chamber design, and only varying the properties of the reinforced layer (Figure S8, Supporting Information).

We developed one actuator (A1) with no reinforced layer, and another actuator (A2) with a thin, textile-based reinforced layer. By combining A1 with each of the two designs of the locally-controllable reinforced layer (L1 and L2), we obtained two further actuators (A3 and A4, respectively). To ensure complete adhesion between the active reinforced layer and the actuators, we first manufactured the actuator with the connected, empty reinforced layer and subsequently filled the chambers with the hydrogel (Figure S9, Supporting Information).

The first series of experiments was performed to evaluate the block force produced by the actuation upon pressurization (Figure 4B). Due to their small size and thin wall (2 mm), a pressure of 10 kPa was sufficient to bend the actuator. Increasing the pressure to $>15 \text{ kPa}$, instead, produced unstable inflation which caused the chambers to explode. We thus evaluated the performance of the actuators using this range of values for the input pressure. Upon pressurization, as expected, without reinforcement, A1 was in the lowest blocking force (9.8 mN). The lack of an inextensible layer and the fact that all the walls had the same thickness prevented the pressure from being moved along a single direction, and instead, the whole actuator expanded. At 10 kPa, A2 showed the best performance. The inextensible layer constrained the pressure so that the upper elastic walls of the actuator expanded thus generating a bending motion. However, when the pressure increased and the controllable inextensible layer was activated, both A3 and A4 had a greater block force than A2. In fact, when all the A3 three sections were active, the actuator provided a 5% higher block force compared to A2. Correspondingly, A4 also provided 27% and 64% higher block forces when two and three sections were activated, respectively.

A second series of experiments was performed to evaluate the resistance of the actuator when pushed in the opposite direction to its actuation motion (Figure 4C). As in the previous case, we measured the resistive force upon pressurization at 10 and 15 kPa while pushing against actuation for 15 mm at a constant speed of 0.7 mm s^{-1} . Overall, actuators A3 and A4 gave the best results at higher pressurization. On average, A3 and A4 showed a 94% higher resistive force than A2, and a 176% higher resistive force than A1.

When all the sections of the controllable actuators were activated, the reinforced layer was stiffened, thus preventing the actuators from bending (Movie S4, Supporting Information). Consequently, the load cell was only in contact with the actuator for the last 3–5 mm of displacement (Figure 4D). The lack of full bending in the fully activated state suggests that the reinforced layer not only changes the bending forces but also enables the soft structure to be maintained in a certain position.

To further prove the stiffening capabilities of the actuators, we performed the following series of compression tests (Figure 4E, left panel). The A3 and A4 actuators were placed in a vertical orientation and were compressed from the top downwards with a given force, while sequentially activating each of their sections. The results showed that the geometry of the inextensible layer plays a major role in absorbing the applied forces.

This is clearly demonstrated by the results for A3 which highlighted that, by increasing the number of active sections, the measured force increases by almost 50% with respect to the initial value, reaching up to 0.74 N. In contrast, the results for A4 showed that the measured force increases only by 3% compared to the initial value. As expected, this confirmed that the behavior is mainly related to the geometry of the pouches and only partially due to the stiffened sections (Movie S5, Supporting Information). However, in order to operate, the actuator needs to be pressurized and this greatly changes its behavior (Figure 4E, right panel). As a consequence of pressurization, the actuator can initially withstand a compression force of only 1.22 and 1.56 N for A3 and A4, respectively, when no section of the reinforced layer is active. However, when the transition phase of the hydrogel in all the sections is activated, the forces increase and reach 2.04 N for A3 and 1.99 N for A4, respectively, showing an increase in their performance of up to 160%.

2.4. Actuator Demonstration

We demonstrated the locally-controllable actuator as part of a gripper using it in different configurations to validate the experimental results and the potential of the combination of materials for future soft robotics applications.

The soft gripper consists of three locally-controllable actuators (A4 type) at an angle of 120° towards each other (Figure 5A). We tested the performance of the actuators by comparing the grasping force in the following cases: i) without activating the reinforced layer, ii) when the rear two sections are activated, iii) when the front section is activated, and iv) when all the three sections are activated. In all the experiments, we performed measurements by positioning the gripper over the target and pressurizing each actuator with 15 kPa. We then pulled the gripper to 25 mm upwards at a constant speed of 0.5 mm s^{-1} and we measured the gripping force.

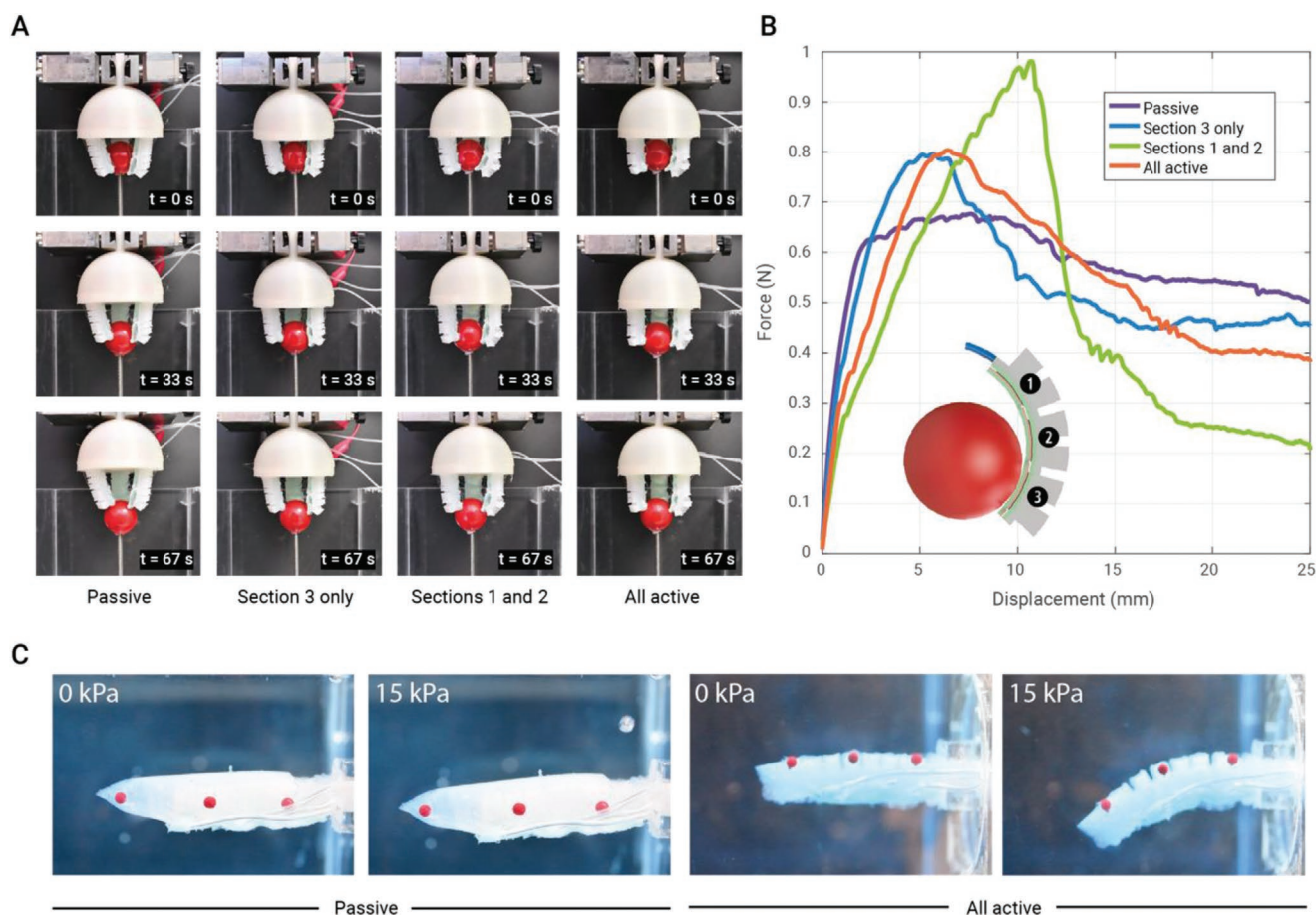


Figure 5. Performance of the soft actuator. A) Performance of three locally controllably soft actuators in a gripper configuration. B) Gripping force as a function of displacement shows that, by activating the two rear sections of the locally controllably inextensible layer, the performance of the gripper improves by more than 100%. C) Performance of the soft actuator in an underwater scenario. By completely stiffening the reinforced layer it is possible to achieve higher bending that can generate variable thrusts if the proposed method is used in a soft underwater propulsion mechanisms.

The results showed that the use of a single section (front one) and the full activation of the reinforced layer only led to a minimal increase in the gripping force (18.2 N on average). Instead, by actuating the rear section and the central section together, there was a 45% increase in gripping force. This configuration bends the tip of the actuator, which greatly improves the adaptation of the gripper to a spherical target, thus increasing the gripping force (Figure 5B, Movie S6, Supporting Information).

We tested the stiffness changing capabilities of the soft actuator in an underwater scenario to expand the possible application opportunities (Figure 5C). Then, we evaluated its performance by comparing the displacement that is achieved when the reinforced layer is activated and when not. In the experiment, the actuator is pressurized (15 kPa) and de-pressurized in sequence to obtain a recoil motion of the soft actuator (Video S7). Results show that when activated, the hydrogel can still create enough stiffness to induce the bending of the actuator upon pressurization. When compared to previous results, the functionalities and the stiffening of the hydrogel-filled layer remain unaltered. However, due to the different density of the medium, the maximum bending angle is reduced (from 56° in the air to 32° in water), an issue that can be solved by increasing the input pressure.

3. Conclusions

The introduction of soft materials in robotics has led to a new class of machines that are more compliant and versatile, and enable a safer interaction with the environment. However, to further improve their adaptive behavior, these robots need to be built and actuated with materials that can reversibly change their elastic properties.

In this work we have presented a novel class of actuators that can tune their properties on demand and thus adapt their behavior. To achieve this goal, we incorporated a thermo-responsive hydrogel (i.e., PNIPAm) into a soft elastic body of a pneumatic actuator to enable triggerable phase transition and selectively and locally control its stiffness.

We therefore verified the related changes in the actuation properties as a consequence of the stiffening of the reinforced layer. The coupling between shape actuation and stiffness tuning of the actuator occurs only in the activated state when the stiffness change of the hydrogel layer affects the shape actuation produced by pressurization. It is not possible to achieve any deformation by simply stiffening the reinforced layer or to achieve bending when the hydrogel-filled layer is in the non-activated state. Similarly, the stiffening of the actuator

can be only achieved as a combination of the two. As shown in Figure 4E, when the hydrogel is activated in absence of any input pressure, the actuator collapses upon compression. Differently, when pressurized, the actuator can withstand up to twice the force which prevents the actuator from collapsing. When completely stiffened, the actuator had a 160% increase in performance when compared to a textile-reinforced PneuNet of the same dimensions. In addition, we found that soft actuators filled with PNIPAm are more effective than those using other materials, such as water and silicone rubber, since this hydrogel has a low mass weight, requires low energy to trigger its reversible phase change, and is locally controllable.

We further evaluated the performance of the PNIPAm-based actuators using them to actuate a soft gripper in an underwater scenario. We evaluated performance of the actuators by selectively activating the various sections of the PNIPAm-based in order to adapt their shape to better conform to the object. By stiffening the rear portion of the actuator and thus forcing the bending point at the tip level, the gripper produced a 130% higher gripping force compared to its inactivated state. Similarly, in when used underwater, by actively controlling the reinforced section of the actuator it was possible to achieve different, controllable bending thus suggesting the use of the proposed approach to enable the development of future controllable stiffening and actuation mechanisms for underwater applications.

The results show that our approach facilitates the development of new actuators that can be controlled for partial or total stiffening and that can create a bending point in continuous structures to exert the required force for a given task. However, to further extend the approach to other robotics applications, the scalability and effectiveness of the PNIPAm-based actuators need to be investigated in different configurations.

One of the main limitations of the current design is the method used to trigger the phase change of the hydrogel. We proved that Joule heating is the most effective method to provide the localized heating required. However, the use of resistive wires revealed some limitations in the manufacturing phase and assembly of the actuators. One solution, still under study, is to replace the wires with an integrated heating system with similar mechanical properties to the materials used to manufacture the actuator. Another key aspect to consider is the effect of the environment on the phase triggering of the material (Video S2, Supporting Information). For this reason, to avoid any unwanted effect due to the environment, the proposed solution can be only used in low-temperature environments (below 40 °C) or in underwater scenarios. Despite this limitation, we believe that our approach opens the way to a new generation of soft machines whose properties can be selectively controlled and thus are better adapted to complex environments.

4. Experimental Section

Materials: N-isopropylacrylamide (NIPAm), N,N'-methylene-bisacrylamide (MBA), ammonium persulfate (APS), and N,N,N',N'-tetramethylethylenediamine (TEMED) were purchased from Sigma-Aldrich. Water in all the experiments was obtained from a Milli-Q water purification system (Merck).

Synthesis and Fabrication of the Hydrogel: The hydrogel used in this work was synthesized following the protocol in Ref. [53] In short, to prepare 25 mL of hydrogel, 2 g of NIPAm were dissolved in 20 mL of millipore water. Then, 0.2% of MBA was added to the solution and dissolved by vortexing for a few seconds. After mixing, the monomer solution was kept on ice for at least 10 min. Initiator APS, 50 mg, was dissolved in 3 mL of millipore water. After positioning the monomer solution in the final mold, 1500 μ L of APS solution and 150 μ L of the accelerator TEMED were mixed with the monomer solution. Polymerization was carried out at 4 °C overnight. The resulting hydrogel was removed from the mold and washed extensively three times in millipore water.

Rheological Characterization: For the rheological characterization, an Anton Paar MCR 302 modular compact rheometer was used, equipped with a double plate of 24.98 mm diameter and a gap of 500 μ m. The hydrogels were loaded into the rheometer as hydrogel at $T = 25$ °C. The samples were then heated to $T = 50$ °C (1 °C min^{-1}). The complex shear modulus G^* at each temperature was measured through an oscillatory test with an amplitude $\gamma = 0.1\%$ and a frequency $\omega = 1$ rad s^{-1} .

Measurements of Thermal Behavior of the Hydrogel: An IR thermal camera (A3255C, FLIR Systems) was used to measure temperatures during the material characterization and to verify the correct internal temperature inside the locally controllable soft actuator.

Measurements of Effects of the External Environment on the Hydrogel: The same volume of hydrogel was placed in a petri dish and in an elastomeric container (the reinforced layer of the actuator) in climatic test chamber (CTS 256, Buch Holm) which was set to cyclically change the temperature from 20 to 50 °C while keeping constant the humidity level (set to 30%, 50%, or 70%). The hydrogel was weighted before and after each test to estimate the weight loss of the material due to the interaction with the environment.

Mechanical Characterization of the Hydrogel and Other Filler Materials: All measurements were taken at room temperature (≈ 27 °C). Vertical indentation tests were performed on the hydrogel and the soft cylindrical cylinder by using a linear stage (M-111 Compact Micro-Translation Stage, PI). A 6-DOF load cell (Nano17, ATI), with the +X axis pointing upward, was fixed to the slider and used to acquire the measurements. Before each measurement, the readings of the load cell were offset to provide a common reference. For all the experiments, measurements were repeated at least five times.

Indentation Tests on the Hydrogel: Indentation force measurements were performed on the gel using a circular probe (38.5 mm² surface area). Before the test, the hydrogel was removed from the fridge (4 °C) and left at room temperature until the temperature was equilibrated. To measure the force of the activated hydrogel, it was placed over a hot plate (50 °C) until the phase transition was reached and then placed under the load cell.

Indentation Test on the Soft Cylinders: The measurements were performed using a square probe (40 mm² surface area). All the cylinders were filled with the same volume of material using a syringe. Due to the thermal resistivity of the silicone rubber, the phase transition in the hydrogel cannot be induced by external heating, thus Joule heating was used.

Three-Point Bending Tests: For the measurements, a dedicated setup was 3D-printed consisting of support pillars and the indenter. The pillars were firmly attached to the reference surface, and the indenter was screwed directly to the load cell.

Mechanical Characterization of the Selectively Inextensible Layer and the Actuators: All the measurements were performed at room temperature (≈ 27 °C) and were acquired using the same linear stage and 6-DOF load cell used for the previous characterizations. All force measurements followed the same protocol: the load cell readings were offset and at least five repetitions were made.

Block Force of the Actuator: The actuator was fixed at the same height as the support connected to the load cell (40 mm² surface) and at a sufficient distance to enable the tip to touch the center of the support. The force was measured during pressurization. Before each pressurization (10, 15 kPa), the actuator was depressurized to avoid errors in the measurements.

Vertical Pushing of the Actuator: The measurements were taken in the same configuration as for measuring the blocking force. The linear stage was then moved downwards by 15 mm and the actuator was left to follow its movement by gravity while measuring the force. Force measurements were offset again before the start of the experiment.

Stiffening Force of the Actuator: The actuator was fixed vertically under the load cell in a configuration in which only the lower part of the actuator was in contact with the probe (square probe, 40 mm² surface area). Then, after offsetting its measurements, the load cell was moved vertically towards the actuator and the force was measured.

Vertical Pushing of the Controllable Inextensible Layer: The controllable inextensible layers were fixed at the same height as the support connected to the load cell (40 mm² surface) and at a sufficient distance to enable the tip of the inextensible layers to touch the border of the support. Before performing the measurements of the activated section, the layers were each Joule heated for 60 s.

Grasping Test: For the grasping test, a gripper was fabricated with three fingers oriented at 120° from each other. Each finger consisted of a PneuNet actuator (A1) with a locally controllable inextensible layer (L2). Actuation was performed by a single channel connected to a compressor. The internal pressure of the actuators was measured, and an external measuring board was used to maintain the exact pressure in the system. As a target, a small spherical object (35 mm in diameter) fixed to a 100 N load cell (Zwick/Roell) was used. When in position, the various sections of the inextensible layer were activated and then the actuator was pressurized. The gripper was fixed to a static measurement device (Z005, Zwick/Roell), which was used to move the gripper upwards and to measure the gripping force. Measurements for all the configurations were taken at least five times.

Data and Image Processing: All the data acquired during the experiments were stored in CSV format. To process the data, a series of MATLAB (MATLAB 2019a, MathWorks Inc.) scripts was developed to extract and process the numerical data acquired.

Supporting Information

Supporting Information is available from the Wiley Online Library or from the author.

Acknowledgements

The authors would like to thank Dr. Francesca Pignatelli for performing the thermal and rheological analyses on the hydrogel.

Conflict of Interest

The authors declare no conflict of interest.

Author Contributions

F.V. conceived the idea, performed the initial synthesis of the hydrogel, designed, and performed the experiments, analyzed the data, and wrote the manuscript. S.P.M.B designed and manufactured the actuators and the silicone pouches, performed the experiments, and contributed to the manuscript. F.M. performed the synthesis of the hydrogel and contributed to the manuscript. B.M. supervised the whole work and contributed to the manuscript.

Data Availability Statement

The data that support the findings of this study are available from the corresponding author upon reasonable request.

Keywords

hydrogels, local-controllable actuators, selective-configuration, soft robotics

Received: February 3, 2021

Revised: April 21, 2021

Published online:

- [1] B. Mazzolai, C. Laschi, *Sci. Rob.* **2020**, 5, eaba6893.
- [2] C. Laschi, M. Cianchetti, *Front. Bioeng. Biotechnol.* **2014**, 2, 3.
- [3] A. Sadeghi, E. Del Dottore, A. Mondini, B. Mazzolai, *Soft Rob.* **2020**, 7, 85.
- [4] E. W. Hawkes, L. H. Blumenschein, J. D. Greer, A. M. Okamura, *Sci. Rob.* **2017**, 2, eaan3028.
- [5] D. S. Shah, J. P. Powers, L. G. Tilton, S. Kriegman, J. Bongard, R. Kramer-Bottiglio, *Nat. Machine Intell.* **2021**, 3, 51.
- [6] H. Abidi, M. Cianchetti, *Front. Rob. AI* **2017**, 4, 5.
- [7] A. Alspach, J. Kim, K. Yamane, in *2018 IEEE Int. Conf. on Soft Robotics (RoboSoft)*, IEEE, Livorno, Italy **2018**, p. 369.
- [8] J. Hughes, U. Culha, F. Giardina, F. Guenther, A. Rosendo, F. Iida, *Front. Rob. AI* **2016**, 3, 69.
- [9] J. Shintake, V. Cacucciolo, D. Floreano, H. Shea, *Adv. Mater.* **2018**, 30, 1707035.
- [10] S. P. M. Babu, F. Visentin, A. Sadeghi, A. Mondini, B. Mazzolai, *IEEE Rob. Autom. Lett.* **2020**, 5, 4055.
- [11] J. M. Florez, B. Shih, Y. Bai, J. K. Paik, in *2014 IEEE Int. Conf. on Robotics and Biomimetics (ROBIO)*, IEEE, Bali, Indonesia **2014**, p. 27.
- [12] J. Guo, C. Xiang, A. Conn, J. Rossiter, *Soft Rob.* **2020**, 7, 309.
- [13] Y. Yang, Y. A. Tse, Y. Zhang, Z. Kan, M. Y. Wang, in *2019 2nd IEEE Int. Conf. on Soft Robotics (RoboSoft)*, IEEE, Seoul, Korea **2019**, p. 161.
- [14] M. Calisti, in *Soft Robotics: Trends, Applications and Challenges* (Eds: C. Laschi, J. Rossiter, F. Iida, M. Cianchetti, L. Margheri), Springer International Publishing, Cham **2017**, pp. 31–36.
- [15] C. A. Aubin, S. Choudhury, R. Jerch, L. A. Archer, J. H. Pikul, R. F. Shepherd, *Nature* **2019**, 571, 51.
- [16] H. Feng, Y. Sun, P. A. Todd, H. P. Lee, *Soft Rob.* **2020**, 7, 233.
- [17] B. Mazzolai, A. Mondini, F. Tramaccere, G. Riccomi, A. Sadeghi, G. Giordano, E. Del Dottore, M. Scaccia, M. Zampato, S. Carminati, *Adv. Intell. Syst.* **2019**, 1, 1900041.
- [18] S. I. Rich, R. J. Wood, C. Majidi, *Nat. Electron.* **2018**, 1, 102.
- [19] M. Cianchetti, M. Calisti, L. Margheri, M. Kuba, C. Laschi, *Bioinspir. Biomim.* **2015**, 10, 035003.
- [20] Y. Wu, J. K. Yim, J. Liang, Z. Shao, M. Qi, J. Zhong, Z. Luo, X. Yan, M. Zhang, X. Wang, R. S. Fearing, R. J. Full, L. Lin, *Sci. Rob.* **2019**, 4, eaax1594.
- [21] M. Kruusmaa, P. Fiorini, W. Megill, M. de Vittorio, O. Akanyeti, F. Visentin, L. Chambers, H. E. Daou, M. Fiazza, J. Ježov, M. Listak, L. Rossi, T. Salumae, G. Toming, R. Venturelli, D. S. Jung, J. Brown, F. Rizzi, A. Qaltieri, J. L. Maud, A. Liszewski, *IEEE Rob. Autom. Mag.* **2014**, 21, 51.
- [22] E. Sinibaldi, A. Argiolas, G. L. Puleo, B. Mazzolai, *PLoS One* **2014**, 9, e102461.
- [23] L. Margheri, C. Laschi, B. Mazzolai, *Bioinspir. Biomim.* **2012**, 7, 025004.
- [24] C. Laschi, B. Mazzolai, V. Mattoli, M. Cianchetti, P. Dario, in *Experimental Robotics* (Eds: O. Khatib, V. Kumar, G. J. Pappas), Springer, Berlin **2009**, p. 25–33.
- [25] Y. Yekutieli, G. Sumbre, T. Flash, B. Hochner, *Biologist* **2002**, 49, 250.
- [26] A. Johnsson, V. K. Sharma, W. Engelmann, in *Plant Electrophysiology: Signaling and Responses* (Ed: A. G. Volkov), Springer, Berlin **2012**, p. 85.

- [27] S. Y. Kim, R. Baines, J. Booth, N. Vasios, K. Bertoldi, R. Kramer-Bottiglio, *Nat. Commun.* **2019**, *10*, 3464.
- [28] D. Lunni, M. Cianchetti, C. Filippeschi, E. Sinibaldi, B. Mazzolai, *Adv. Mater. Interfaces* **2020**, *7*, 1901310.
- [29] J. Shintake, B. Schubert, S. Rosset, H. Shea, D. Floreano, in *2015 IEEE/RSJ Int. Conf. on Intelligent Robots and Systems (IROS)*, IEEE, Hamburg, Germany **2015**, pp. 1097.
- [30] T. Chenal, J. C. Case, J. K. Paik, R. K. Kramer, *2014 IEEE/RSJ Int. Conf. on Intelligent Robots and Systems*, IEEE, Chicago, IL **2014**, 2827.
- [31] A. Ogawa, G. Obinata, K. Hase, A. Dutta, M. Nakagawa, *Conf. Proc. IEEE Eng. Med. Biol. Soc.* **2008**, *2008*, 330.
- [32] W. Shan, T. Lu, C. Majidi, *Smart Mater. Struct.* **2013**, *22*, 085005.
- [33] M. Langer, E. Amanov, J. Burgner-Kahrs, *Soft Rob.* **2018**, *5*, 291.
- [34] J. A.-C. Liu, J. H. Gillen, S. R. Mishra, B. A. Evans, J. B. Tracy, *Sci. Adv.* **2019**, *5*, eaaw2897.
- [35] L. Blanc, A. Delchambre, P. Lambert, *Actuators* **2017**, *6*, 23.
- [36] K. Tanaka, M. A. Karimi, B. Busque, D. Mulroy, Q. Zhou, R. Batra, A. Srivastava, H. M. Jaeger, M. Spenko, in *2020 3rd IEEE Int. Conf. on Soft Robotics (RoboSoft)*, IEEE, New Haven, CT **2020**, p. 852.
- [37] E. Steltz, A. Mozeika, J. Rembisz, N. Corson, H. M. Jaeger, in *Electroactive Polymer Actuators and Devices (EAPAD) 2010* (Ed: Y. Bar-Cohen), SPIE, Bellingham, Washington **2010**, p. 640–648.
- [38] Y. Lin, J. Zou, H. Yang, in *Intelligent Robotics and Applications* (Eds: H. Yu, J. Liu, L. Liu, Z. Ju, Y. Liu, D. Zhou), Springer International Publishing, Cham **2019**, pp. 531–543.
- [39] M. Ibrahimi, L. Paternò, L. Ricotti, A. Menciassi, *Soft Rob.* **2020**, *8*, 85.
- [40] V. Wall, R. Deimel, O. Brock, in *2015 IEEE Int. Conf. on Robotics and Automation (ICRA)*, IEEE, Seattle **2015**, p. 252.
- [41] A. Sadeghi, A. Mondini, B. Mazzolai, *Actuators* **2019**, *8*, 47.
- [42] M. A. Robertson, J. Paik, *Sci. Rob.* **2017**, *2*, eaan6357.
- [43] Y. Cao, G. Zhang, Y. Zhang, M. Yue, Y. Chen, S. Cai, T. Xie, X. Feng, *Adv. Funct. Mater.* **2018**, *28*, 1804604.
- [44] M. Cai, S. Nie, Y. Du, C. Wang, J. Song, *ACS Appl. Mater. Interfaces* **2019**, *11*, 14340.
- [45] H. Liu, M. Li, S. Liu, P. Jia, X. Guo, S. Feng, T. J. Lu, H. Yang, F. Li, F. Xu, *Mater. Horiz.* **2020**, *7*, 203.
- [46] Y. Zhao, C. Xuan, X. Qian, Y. Alsaïd, M. Hua, L. Jin, X. He, *Sci. Rob.* **2019**, *4*, eaax7112.
- [47] C. Li, G. C. Lau, H. Yuan, A. Aggarwal, V. L. Dominguez, S. Liu, H. Sai, L. C. Palmer, N. A. Sather, T. J. Pearson, D. E. Freedman, P. K. Amiri, M. O. de la Cruz, S. I. Stupp, *Sci. Rob.* **2020**, *5*, eabb9822.
- [48] F. Ilievski, A. D. Mazzeo, R. F. Shepherd, X. Chen, G. M. Whitesides, *Angew. Chem., Int. Ed.* **2011**, *50*, 1890.
- [49] K. Ogura, S. Wakimoto, K. Suzumori, Y. Nishioka, in *2008 IEEE Int. Conf. on Robotics and Biomimetics*, IEEE, Bangkok, Thailand **2009**, pp. 462.
- [50] Y. Hirokawa, T. Tanaka, *J. Chem. Phys.* **2020**, *81*, 6379.
- [51] Y. Yu, B. D. Kieviet, F. Liu, I. Siretanu, E. Kutnyánszky, G. J. Vancso, S. de Beer, *Soft Matter* **2015**, *11*, 8508.
- [52] Z. Ahmed, E. A. Gooding, K. V. Pimenov, L. Wang, S. A. Asher, *J. Phys. Chem. B* **2009**, *113*, 4248.
- [53] C. Wang, N. T. Flynn, R. Langer, *Adv. Mater.* **2004**, *16*, 1074.
- [54] S. R. Sershen, S. L. Westcott, N. J. Halas, J. L. West, *J. Biomed. Mater. Res.* **2020**, *51*, 293.
- [55] Y. Guan, Y. Zhang, *Soft Matter* **2011**, *7*, 6375.
- [56] V. Pardo-Yissar, R. Gabai, A. N. Shipway, T. Bourenko, I. Willner, *Adv. Mater.* **2020**, *13*, 1320.
- [57] J. M. Weissman, H. B. Sunkara, A. S. Tse, S. A. Asher, *Science* **1996**, *274*, 959.
- [58] Y.-J. Lee, P. V. Braun, *Adv. Mater.* **2003**, *15*, 563.
- [59] A. K. Mishra, T. J. Wallin, W. Pan, P. Xu, K. Wang, E. P. Giannelis, B. Mazzolai, R. F. Shepherd, *Sci. Rob.* **2020**, *5*, eaaz3918.
- [60] J. Kim, S. Nayak, L. A. Lyon, *J. Am. Chem. Soc.* **2005**, *127*, 9588.
- [61] V. Miruchna, R. Walter, D. Lindlbauer, M. Lehmann, R. von Klitzing, J. Müller, in *Proc. of the 28th Annual ACM Symp. on User Interface Software & Technology*, Association For Computing Machinery, New York **2015**, pp. 3–10.
- [62] M. Stieger, J. S. Pedersen, P. Lindner, W. Richtering, *Langmuir* **2004**, *20*, 7283.
- [63] C. Majidi, *Soft Rob.* **2014**, *1*, 5.
- [64] K. Gawlitza, S. T. Turner, F. Polzer, S. Wellert, M. Karg, P. Mulvaney, R. von Klitzing, *Phys. Chem. Chem. Phys.* **2013**, *15*, 15623.